Laser Induced Breakdown Spectroscopy of RDX and HMX with nanosecond, picosecond, and femtosecond pulses

S. Sreedhar, M. Ashwin Kumar, G. Manoj Kumar, # P. Prem Kiran, Surya P. Tewari, S. Venugopal Rao

Advanced Centre of Research in High Energy Materials **(ACRHEM)**
University of Hyderabad, Hyderabad 500046, India.

 # Author for correspondence e-mail: manojsp@uohyd.ernet.in

ABSTRACT

Herein we present some of our initial experimental results obtained from the laser induced breakdown spectroscopic (LIBS) measurements of RDX and HMX using nanosecond (ns), picosecond (ps), and femtosecond (fs) laser pulses acquired without gating and delay. RDX and HMX were mixed with KBr and pellets were prepared for the spectroscopic studies. Nanosecond pulses at 532 nm, ps/fs pulses at 800 nm were used for the experiments. The spectra were collected using Ocean Optics 4000/Maya spectrometer using a UV transmitting, 400 μm core diameter fiber in one case and a combination of lenses to collect the light from plasma in the second case. Several features were observed in the spectra exclusive for each pulse domain. The differences/similarities in the spectra collected using different pulses are presented.

Key words: LIBS, RDX, HMX, nanosecond, picosecond, femtosecond.

1. INTRODUCTION

Investigating and understanding different techniques for accomplishing practical devices that can detect various high energy materials such as RDX, HMX, etc. has been the priority of many scientists over the last decade [1-6]. The desirable features of such devices are (a) portability: detection can be on the move (b) versatility: distinguish between an explosive and non-explosive thereby eliminating false alarms (c) stand-off capability: detection from a distance (few tens of metres) to avoid hazardous materials (d) quick analyzing time: ability to identify the threat immediately in order to prevent or minimize the damage (e) cost effective. Several techniques (radiation based and vapor sensing based) till date have been investigated including (a) Raman processes (b) fluorescence quenching (c) nuclear quadrupole resonance spectroscopy (d) ion mobility spectrometry (e) terahertz spectroscopy and (f) laser induced breakdown spectroscopy (LIBS) etc. [7-21]. Laser Induced Breakdown Spectroscopy (LIBS) is a rapid chemical analysis technology that uses a short laser pulse to create a micro-plasma on the sample surface [18-24]. This analytical technique offers many compelling advantages compared to other elemental analysis techniques. These include:

- A sample preparation-free measurement technique
- Extremely fast measurement time, usually a few seconds, for a single analysis
- Broad elemental coverage, including lighter elements, such as H, C, N, O, Na etc.
- Versatile sampling protocols that include fast raster of the sample surface and depth profiling
- Thin-sample analysis without the concern of substrate interference

The main physical process that forms the essence of LIBS technology is the formation of high-temperature plasma, induced by a short laser pulse. When the short-pulse laser beam is focused onto the sample surface, a small volume of the sample mass is ablated. This ablated mass further interacts with a trailing portion of the laser pulse to form highly energetic plasma that contains free electrons, excited atoms, and ions. Many studies have proved that the plasma temperature can exceed 30,000 K in its early life time phase. The plasma starts to cool immediately after the laser pulse terminates. During the plasma cooling process electrons of the atoms and ions from excited electronic states recombine causing the plasma to emit light with discrete spectral peaks. Emitted light from the plasma is collected with a spectrograph coupled to an ICCD/array detector module for LIBS spectral analysis. Each element in the periodic table is

Chemical, Biological, Radiological, Nuclear, and Explosives (CBRNE) Sensing XI, edited by Augustus Way Fountain III, Patrick J. Gardner, Proc. of SPIE Vol. 7665, 76650T · © 2010 SPIE · CCC code: 0277-786X/10/$18 · doi: 10.1117/12.850007

associated with unique LIBS spectral peaks. By identifying different peaks for the analyzed samples, chemical composition of the material can be rapidly determined. Information from the LIBS peak intensities can often be used to quantify concentration of trace and major elements in the sample. Based on the spectral intensities and certain analyses stoichiometry of the compound under study can be determined accurately. Several detailed studies in the last few years have resulted in the development of man-portable LIBS and standoff detection up to 100m distances [25-30]. Though LIBS technique has demonstrated the capability to identify HEM's such as RDX, TNT, C4 etc. [31-36] there are several issues, for instance the reliability and infallible nature, which need to be addressed before concluding the significance of this technique compared to others mentioned above. In this context, there have been several studies devoted to (a) analyze the LIBS data accurately using various models and approaches (b) use femtosecond (fs) or picosecond (ps) pulses to identify the potential and advantages over conventional nanosecond (ns) pulse LIBS (c) enhance the signal-to-noise ratio using double pulse techniques etc. [37-42]. Herein we present our initial results on the LIBS measurements of RDX and HMX (embedded in KBr matrix) using ns, ps, and fs pulses. Our short term goal is to understand the physics of ns, ps, and fs pulse interaction with these molecules and later implement the LIBS technique using best pulse width possible for unambiguous detection of high energy materials.

2. EXPERIMENTAL DETAILS

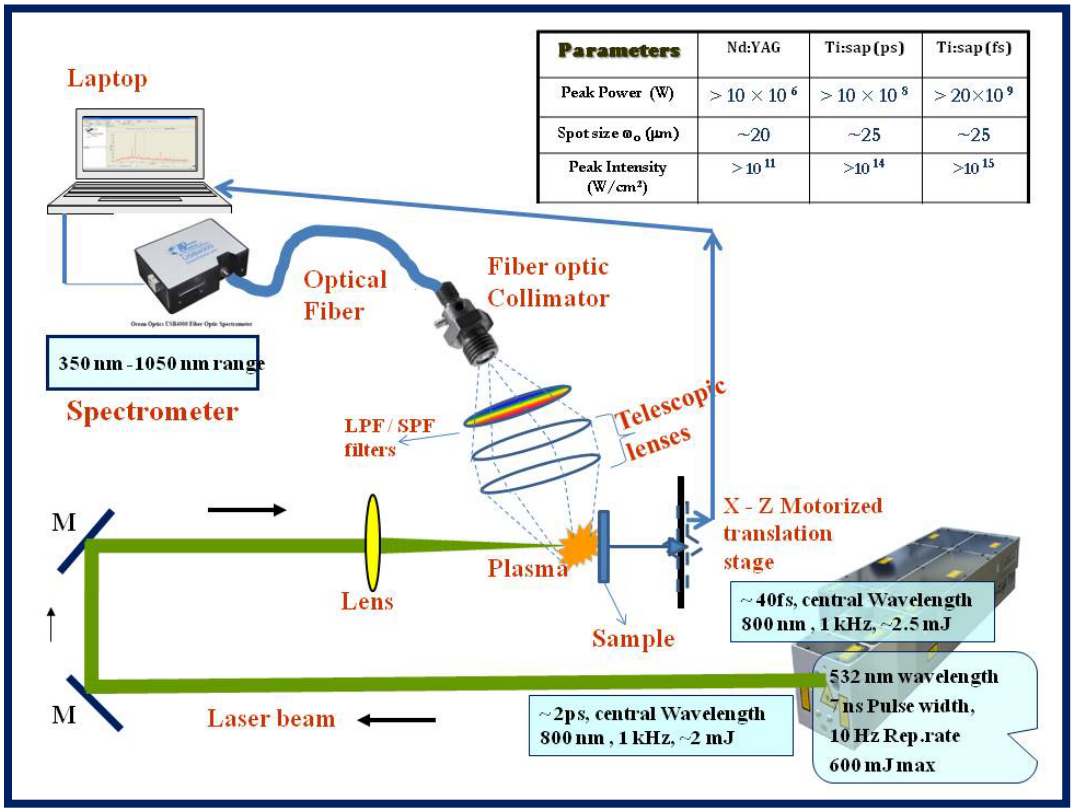

Figure 1 Experimental setup used for collecting LIBS spectra using ns pulses.

Figure 1 illustrates the experimental set up used for recording the LIBS spectrum. Nd:YAG laser pulses at 532 nm of ~7 ns duration, 10 Hz repetition rate and ~6.5 mm spot size with typical energies of 10-20 mJ/pulse were focused using an 80 mm lens on the sample. The beam waist was estimated to be ~20 μm and the corresponding Rayleigh range was estimated to be ~0.5 mm. This corresponds to an intensity of >100 GW/cm^2. The sample was placed approximately 1 mm before the focus (towards the lens) where the spot size 80 μm and intensity was 18 GW/cm^2. As the laser energy increased we observed light and sound coming from the focal region at a particular energy. The breakdown threshold for RDX+KBr and HMX+KBr was <10 GW/Cm^2. As the experiment was executed in ambient air

it was essential to take care of the LIBS signal contribution from it also. The breakdown threshold of air was >50 GW/cm^2 which was well above the breakdown threshold for RDX(HMX)+KBr. The light from the breakdown region was collected using collection lenses of 100 mm and 150 mm placed ~30° to the propagation direction, which in turn was connected to a fiber and a spectrometer (USB 4000 from Ocean Optics; 350-1050 nm). The resolution of spectrometer was ~1.5 nm. The data was collected with 1000 millisecond integration time. The samples were weighed with a micro-balance and mixed with spectroscopic grade KBr (2 g by weight) to arrive at desired concentrations. The mixture is then grinded with agate mortar until it formed a uniform concoction. This powdered mixture was taken into metal circular die of 20 mm diameter. Then a pressure was applied with hydraulic machine up to 9 tonnes approximately over a period of 20 minutes. The pellets thus formed were used for our LIBS experiments.

3. RESULTS AND DISCUSSION

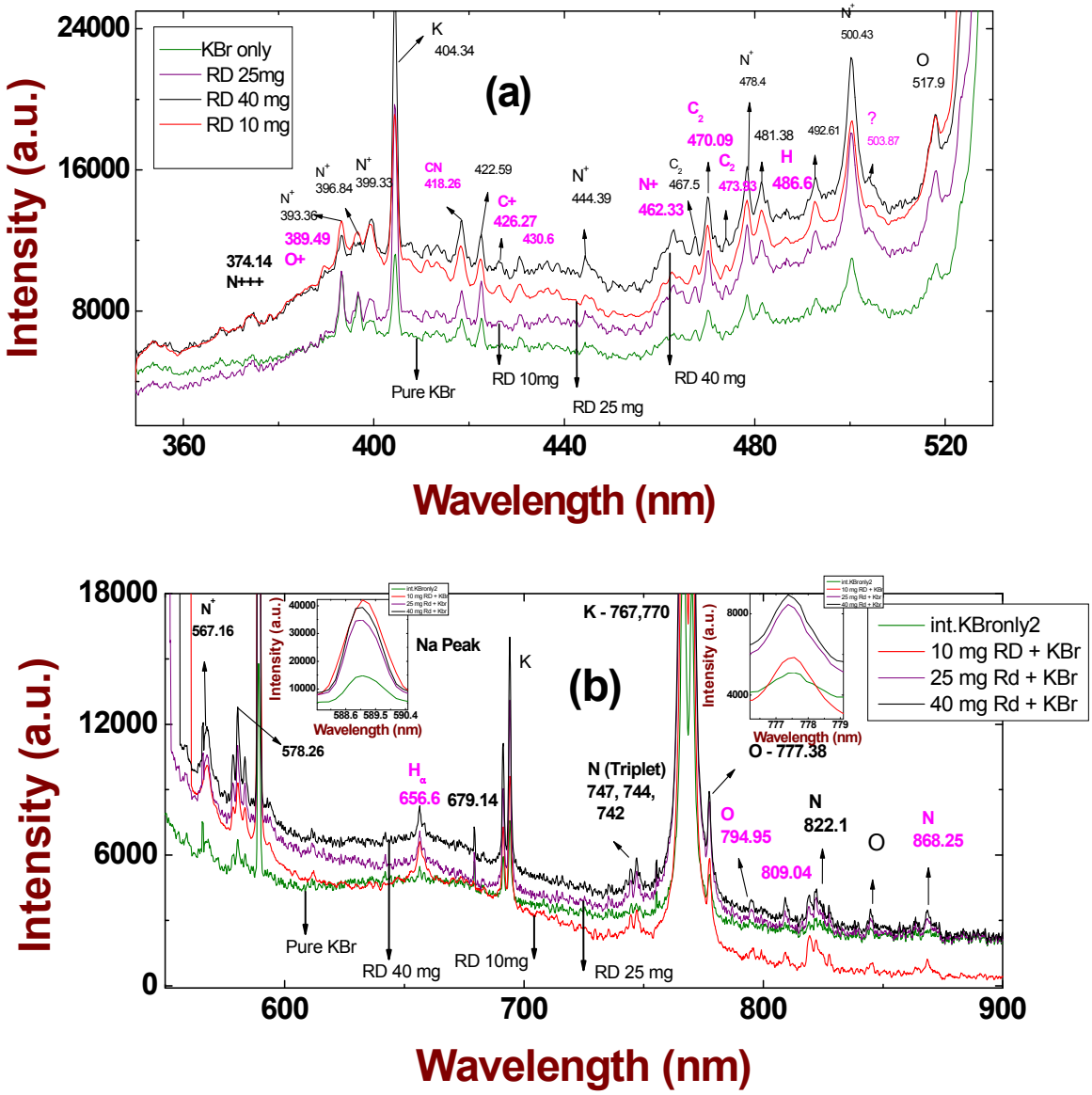

Figure 2 LIBS spectrum of RDX with **ns** pulses in the left (350-525 spectral range) and right (525–900 nm spectral range). The lower spectrum (green color) corresponds to KBr only while the top three spectra correspond to RDX+KBr with increasing concentration or RDX. Input energy used was ~8 mJ.

Figure 2(a) shows typical ns LIBS spectra collected from RDX+KBr with top three curves representing increasing concentration of RDX in KBr (10, 25, and 40 mg in 2 g of KBr) and bottom curve represents spectrum from KBr alone in the spectral range of 350-525 nm. Figure 2(b) shows the second half of the spectrum in the 525-900 nm spectral range. Most of the peaks were assigned using the NIST database [43] while few peaks were not found in the NIST database. Due to the insufficient resolution of the spectrometers used some of the peaks were not resolved and the peak wavelengths matched with the NIST database within 0.5 nm. The peaks indicated in magenta color (bold) were observed exclusively from the RDX+KBr matrix. Several key features observed from the spectra can be summarized as:

1. CN peak at 418.26 nm and C_2 peaks appearance at 467.50 nm, 470.09 nm, and 473.93 nm are attributes of the nitro compounds.
2. Several peaks were observed ONLY for the RDX+KBr mixture. C^+ peak at 426.27 nm was observed exclusively in RDX sample (i.e. we confirmed the observed peaks were not from KBr). N^+ peak at 462.33 nm was observed only in RDX sample while it was clearly absent in the KBr spectrum. Similarly, H_β (486.6 nm), N (868.43 nm), and O (794.95) peaks were exclusively from RDX in the sample.
3. H_α (656.6 nm), O (777.38 nm, 845.6 nm) peaks exhibited enhanced intensity (by at least 4 times) in the RDX+KBr spectrum compared to pure KBr spectrum. N (Triplet) (742.36 nm, 744.64 nm, 747.12 nm) and N (822.1 nm and 868.43 nm) peak intensities were also enhanced in the RDX spectrum. Enhancement was also observed for the sodium doublet peak (589.11 nm). Table II summarizes the peaks observed and the assignment of atomic species to the corresponding spectral lines. The peaks in bold are observed exclusively from RDX.
4. Figure 3 depicts the variation of C_2 peak (470.09 nm), CN peak (418.26 nm), and H_α peak intensities versus the concentration of RDX after deducting the KBr contribution. It is evident that the peak intensities increased as a function of concentration. We ensured that contribution from air was minimal by placing the sample at positions where peak intensities were not sufficient for air breakdown. H_α peak intensity variation did not divulge any trend.

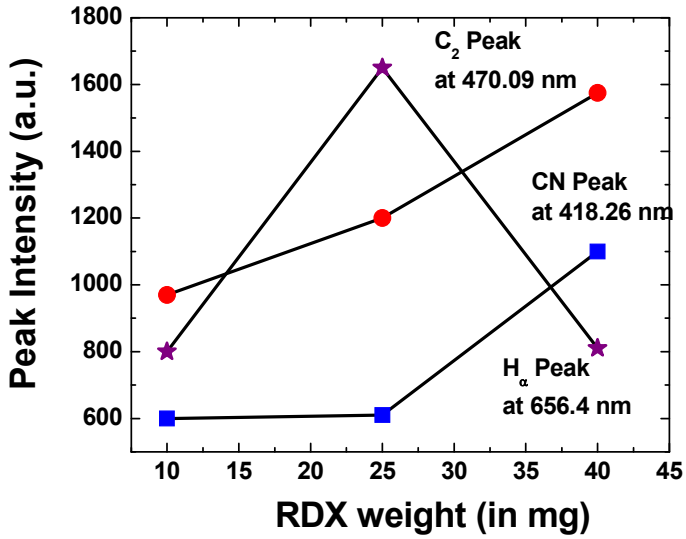

Figure 3 Variation of different peaks observed in RDX LIBS spectrum as a function of concentration.

Several approaches have been explored by carious groups to differentiate the explosives from other organic materials (since both of these contain C, O, N, H etc. and few other impurities). Some of the earlier works concluded (a) the presence of a certain time window in the plasma evolution for which distinguishing explosives from substrates (e.g. Al and plastic) is most favorable (b) partial least squares discrimination analysis of LIBS spectral data provides information about the differentiation of explosives from other organics. The coupling of LIBS data with chemometric techniques is an important tool for classification of explosives [26] (c) earlier LIBS experiments claim that evolution of the concentration of C_2 species in the RDX plasma plume demonstrated double-peak behavior [32]. The initial mechanism of explosive decomposition is not important in determining its signature in the LIBS measurement time window (1–30 μs). Electron-excitation impact processes are mainly responsible for generation of excited states (d) Use

of femtosecond pulses for LIBS experiments [24]. Ultrashort laser pulses offer several advantages over the nanosecond counterparts [14-15]. A few merits include (i) Low ablation threshold resulting from large peak powers and minimum energy dissipation in the sample (ii) Effective ablation due to energy confinement (iii) Less thermal damage to the sample (iv) higher efficiency/reliability. The background is generally bereft of lines arising from the ambient air.

Significant Peaks Observed (nm)	**NIST Reference [43]**
374.14	N^{+++} -374.754
389.49	**O^+ [43]**
393.86	N^+ (393.366)
396.84	N^+ (396.847)
399.33	N+ (399.500)
404.34	K (404.414)
426.27	**C+ (426.72)**
418.26	**CN [41]**
422.59	CN
462.33	**N^+ (462.139)**
467.50	**C_2 [41]**
470.09	**C_2 [41]**
473.93	**C_2 [41]**
500.43	N^+ (500.515)
486.6	**H_β (486.1)**
567.16	N^+ (567.602)
589.11	Na doublet (588.99, 589.5924)
656.4	**H_α (656.2) enhanced by ~4 times**
742, 744.64, 747.12	N (Triplet) (742.364, 744.229 , 746.831)
777.57	O – 777.38
822.1	N – 822.63, 822.314
794.95	**O [43]**
845.6	O - 844.88
868.25	**N - 868.34, 868.61**

Table I Important peaks observed in the ns LIBS spectrum of RDX (KBr) and their assignment.

Figure 4(a) shows a typical ps LIBS spectrum collected from RDX+KBr and figure 4(b) shows the LIBS spectrum of HMX+KBr with a concentration of 100 mg in 1 g of KBr (by weight). The spectra were collected using a single 400 μm core fiber coupled to a spectrometer (MAYA, Ocean optics, <0.5 nm resolution). The repetition rate of the laser was 100 Hz and the integration (collection) time was set to ~30 ms. We could not collect the data with 1 kHz repetition rate. Typical energies used were ~1 mJ. Some of the interesting features observed were:

1. Observation of the C_2 peak at 469.95 (471.4 nm in reference 41) amongst several others in the spectral range as indicated in figure and H_α peak at 656.51 nm in our spectrum. These two peaks along with CN peaks near 380 nm and the C peak at 248 nm are the signatures of RDX/HMX molecules. In our case we could not observe the CN bands near 380 nm and the **C** peak at 248 nm due to the insufficiencies in detection procedures. The spectra were not corrected for the continuum observed and the presence of strong continuum could be the main reason for not observing these peaks. We are now working with a Mechelle 5000 spectrograph coupled to a gated ICCD (DH734, ANDOR) and hopefully will observe these peaks.
2. Observation of the CN peak near 418 nm in both RDX and HMX spectra. The other peaks such as K, Na etc. were observed clearly.
3. The Oxygen triplet at 777 nm and the Nitrogen triplet at 744 nm were not observed since the CCD saturated at those wavelengths due to the strong pump beam. Moreover, due to non-availability of the desired wavelength cutoff filters we could not observe these peaks.

4. We have also observed N^+, O^+, O^{++} in some of the spectra. Certain peaks (e.g. O^+ at 477.74) were missing from the ns spectra while certain peaks (e.g. C^+ at **426.27 nm)** were missing from the ps spectra. The origin of their presence in the short pulse spectra is being investigated further. Detailed studies are necessary to ascertain the similarities and differences between these spectra.
5. Better signal to noise ratio could be achieved with (a) use of a gated ICCD (b) eliminating the pump from the spectra by appropriate use of filters (c) use of fiber bundle rather than a single fiber (d) additional collimation and focusing lenses (UV transparent).

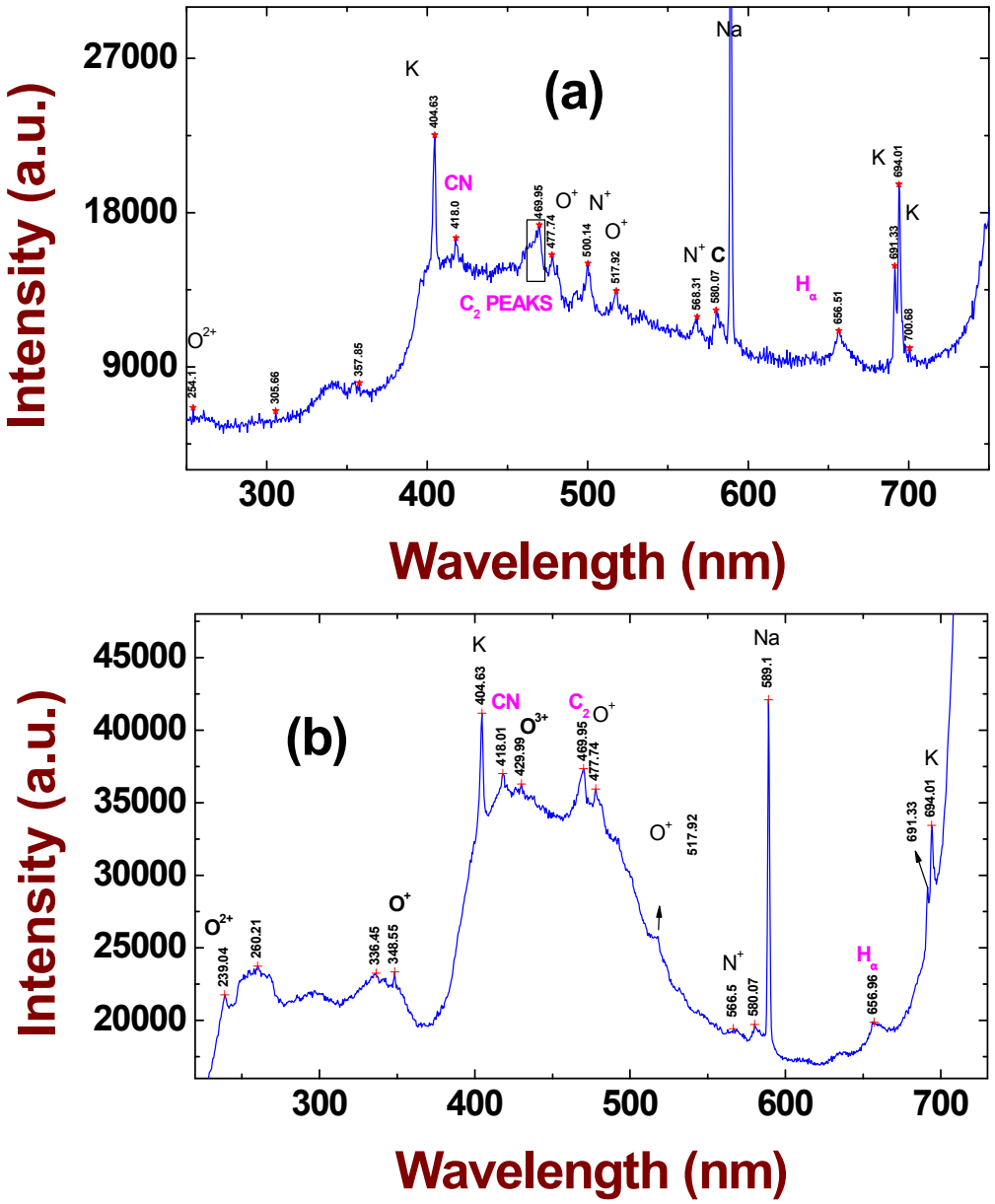

Figure 4 (a) LIBS spectrum of RDX+KBr pellets with **ps** pulses obtained using a bare fiber of 400 μm diameter core. **(b)** LIBS spectrum of HMX+KBr pellets with ps pulses obtained using a bare fiber of 400 μm diameter core.

Figure 5(a) shows a typical fs LIBS spectrum collected from RDX+KBr and figure 5(b) shows the LIBS spectrum of HMX+KBr with a concentration of 100 mg in 1 g of KBr (by weight). The data collection was similar to that of the ps case discussed above. Typical energies used were ~ 1 mJ. The significant attributes of these spectra were:

- Due to non-gated data collection procedure a strong continuum was present in the visible spectral region which hindered the appearance of other smaller intensity peaks.
- C_2 peak appearance at 469.95 nm in both RDX and HMX. Hydrogen peak near 656 nm was also observed.
- Presence of CN peak at ~418 nm.
- Presence of O^{2+} and O^{3+} suggests the pumping with fs pulses have ionized the molecules into extreme excited states.
- Nitrogen (744 nm), Oxygen (777 nm) peaks were not observed due to CCD saturation from the pump intensity.

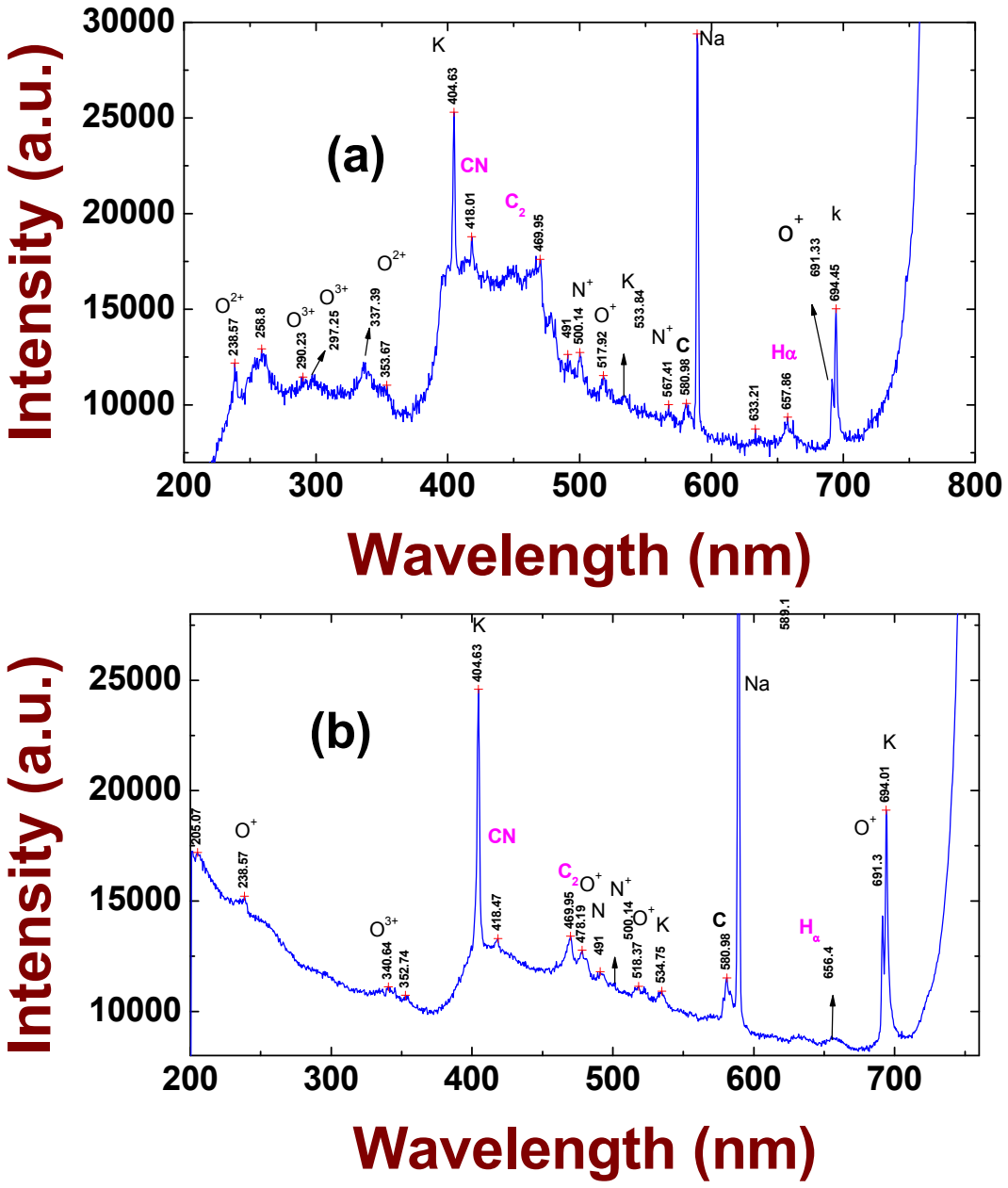

Figure 5 (a) LIBS spectrum of RDX+KBr pellets with **fs** pulses obtained using a bare fiber of 400 µm diameter core **(b)** LIBS spectrum of HMX+KBr pellets with fs pulses obtained using a bare fiber of 400 µm diameter core.

The LIBS spectra with ps and fs pulses were collected using two different procedures. In the first case (described above) a UV transmitting fiber with a core diameter of 400 µm was used to collect the spectra which enabled

us to observe peaks from 250 nm to 1100 nm. In the second case two lenses were used to collimate and focus the light onto a fiber connected to a spectrometer. In this case since the lenses were not UV transparent we could not see the peaks below 350 nm. However, the signal was strong and some of the peaks were resolved nicely.

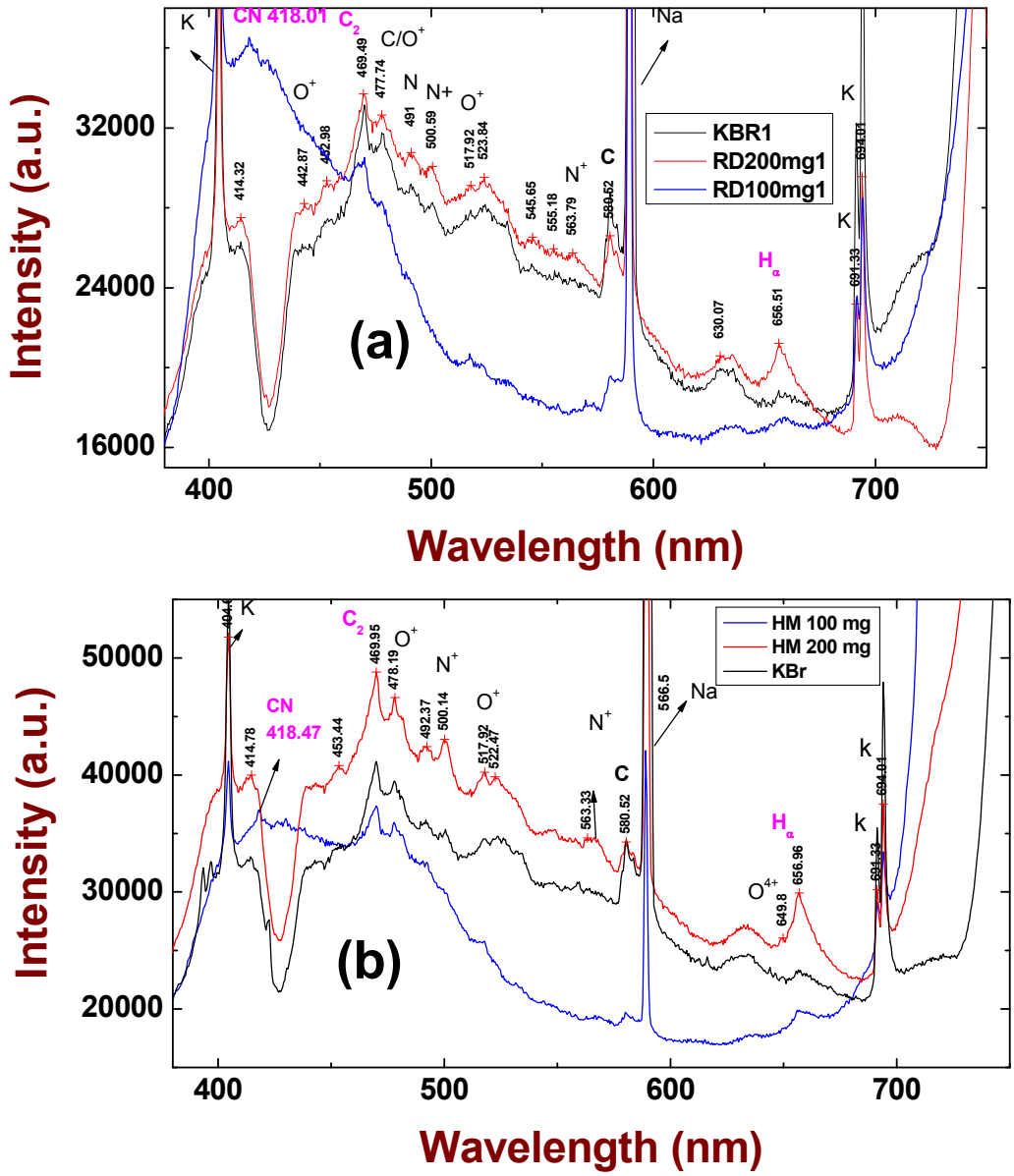

Figure 6 (a) LIBS spectrum of RDX+KBr with **fs** pulses obtained using combination of lenses and MAYA spectrometer. Bottom curve (blue) represents 100 mg of sample in 1 g of KBr, middle curve (black) represents the KBr spectrum, and top curve (red) represents the curve for 200 mg of sample in 800 mg of KBr. **(b)** LIBS spectrum of HMX+KBr pellets with fs pulses. The description of various curves is similar to that of **(a)**.

Figure 6(a) shows typical fs LIBS spectrum collected from RDX+KBr and figure 6(b) shows the spectrum of HMX+KBr with different concentrations of 100/200 mg in 1g/800 mg of KBr. We had increased the concentration of RDX and used the lenses to collect more light from the ps/fs laser induced plasmas. The summary of the peaks observed in both the RDX and HMX spectra is described below.

(a) We had recorded the KBr spectra also at similar experimental conditions which enabled us to decouple the spectra and obtain contributions from RDX or HMX separately.
(b) The H_α peak was enhanced significantly compared to the pure KBr spectrum
(c) The presence of CN peak at 418.01/418.47 is confirmed from RDX/HMX only. C_2 peak at 469.95 was enhanced in RDX/HMX compared to KBr.
(d) The C peak at 248 nm was not observed.
(e) Nitrogen (744 nm), Oxygen (777 nm) peaks were not observed due to CCD saturation from the pump intensity and the non-usage of gated ICCD.

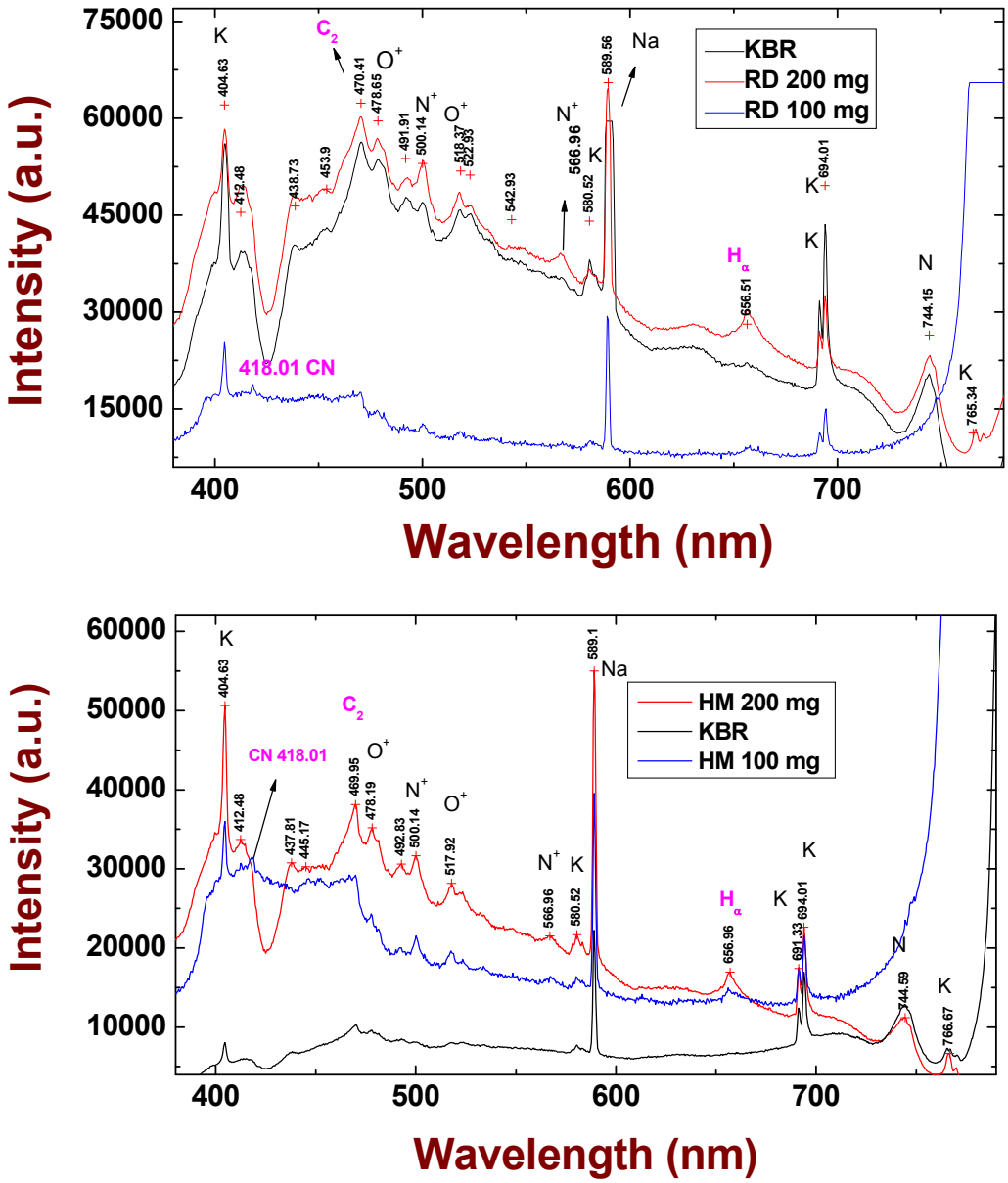

Figure 7(a) LIBS spectrum of RDX+KBr with **ps** pulses obtained using combination of lenses and MAYA spectrometer. Bottom curve (blue) represents 100 mg of sample in 1 g of KBr, middle curve (black) represents the KBr spectrum, and top curve (red) represents the curve for 200 mg of sample in 800 mg of KBr. **(b)** LIBS spectrum of HMX+KBr pellets with fs pulses. Bottom (black) curve is for KBr, middle (blue) for 100 mg of HMX and top (red) for 200 mg of HMX in KBr.

Figure 7(a) shows typical ps LIBS spectrum collected from RDX+KBr and figure 7(b) shows the spectrum of HMX+KBr with different concentrations of 100/200 mg in 1g/800 mg of KBr. Similar to the observations in fs spectra for both of these molecules, H_α and CN were the new peaks along with C_2 peak enhancement was observed in RDX/HMX alone.

These initial studies suggest that further improvements are required to arrive at a conclusion on the similarities and differences of the LIBS spectra collected with ns, ps, and fs pulses. We had performed few initial studies qualitatively to understand the interaction of short pulses with two different HEM's. Our ultimate aim is to bring out the merits/de-merits of using each of these pulses to study high energy materials for practical applications. Various methodologies have been proposed to identify the HEM's from other organic materials using LIBS data Gottfried et al. [41] have demonstrated that the relative elemental intensities in the LIBS spectra are representative of the stoichiometry of parent molecules and can be used to distinguish materials containing the same elements (e.g. RDX and HMX). De Lucia Jr. et al [42] have built the partial least squares discriminant analysis (PLS-DA) model for the LIBS data for explosives detection and iteratively tested it with sample test sets data with good success. Earlier studies on the fs LIBS of RDX [31] suggested the appearance of **C** atomic peak at 248 nm indicates the presence of explosive substance. In contrast, the ns LIBS spectrum illustrated minimal carbon emission. Moreover, they argue the presence of CN molecular fragment at ~ 388 nm is important for identification of the RDX molecule. Weidman et al. [44] performed LIBS experiments by using self-channeled femtosecond pulses and characterized few HEM's. They observed that molecular CN signal was present in the spectrum of organic films even if the sample did not contain nitrogen. They point out that the emission was likely caused by molecular recombination between the carbon atoms in the filament induced plasma and nitrogen in the surrounding atmosphere. Therefore, they feel that CN signal is not a good discriminant between organic materials and explosives, which contain native CN bonds. Several issues (e.g. substrate effects, atmosphere effects, distinguishing between plastics/organics etc.) need to be clarified before attempting to utilize the LIBS technique for field trials [45-47]. However, among the laser based techniques for explosives detection, LIBS still stands out as a unique technique capable of remote detection with a short period of time [48].

4. CONCLUSIONS & FUTURE SCOPE

We had recorded the LIBS spectra of RDX and HMX embedded in a KBr matrix using ns, ps, and fs pulses. The initial results obtained, using a spectrometer without gating and delay, revealed certain features exclusive for each pulse domain. We could observe few of CN and C_2 peaks using ns pulses, which are signatures of nitro-compounds. KBr and impurities present dominated the LIBS spectra with ps and fs pulses.

Our future studies encompass (a) collecting the data with gated ICCD and concentrate on recording the C (248 nm), CN (near 380 nm), and C_2 (near 470 nm) peaks apart from the N, O, H peaks (b) evaluate the O/C, N/C, N/CN etc. ratios (c) record the time dependent evolution of CN/C_2 peaks (d) perform these studies on thin films coated on to a substrate (e.g. Aluminum) using ns, ps, and fs pulses to arrive at the merits of each of these pulses.

ACKNOWLEDGEMENTS

We acknowledge HEMRL, Pune for providing the samples of RDX and HMX. Financial support from DRDO is gratefully acknowledged.

REFERENCES

[1] K. L. McNesby and R. A. Pesce-Rodriguez, "Applications of vibrational spectroscopy in the study of explosives," in Handbook of Vibrational Spectroscopy, J.M. Chalmers, P.R. Griffiths, eds. (Wiley, Chichester, England, 2002).

[2] A. Tsekoun, I. Dunayevskiy, R. Maulini, R. Barron-Jimenez, A. Lyakh, and C.K.N. Patel, "Compact, rapid, and rugged detector of military and improvised explosives based on external grating cavity quantum cascade lasers," Proc. SPIE, 7434, 74340J (2009).

[3] M.B. Pushkarsky, I.G. Dunayevskiy, M. Prasanna, A.G. Tsekoun, R. Go, and C.K.N. Patel, "High sensitivity spectroscopic detection of TNT using continuously tunable CW room temperature high power quantum cascade lasers", Proc. Natl. Acad. Sci. USA **103**, 19630–19634 (2006).

[4] D.S. Moore, "Instrumentation for trace detection of high explosives," Rev. Sci. Instrum. **75(8),** 2499-2512 (2004).
[5] D. Helfinger, T. Arusi-Parpar, Y. Ron, and R. Lavi, "Application of a unique scheme for remote detection of explosives," Opt. Commun. **204(1-6),** 327-331 (2002).
[6] C. M. Wynn, S. Palmacci, R. R. Kunz, J. J. Zayhowski, B. Edwards, and M. Rothschild, "Experimental demonstration of remote detection of trace explosives," Proc. SPIE **6954**, 695407 (2008).
[7] K. Yamamoto, M. Yamaguchi, F. Miyamaru, M. Tani, M. Hangyo, T. Ikeda, A. Matsushita, K. Koide, M. Tatsuno, Y. Minami, "Noninvasive inspection of C-4 Explosive in mails by terahertz time–domain spectroscopy," Jap. J. of Appl. Phys., **43(3)B**, L414-L417 (2004).
[8] J. Moros, J.A. Lorenzo, P. Lucena, L.M. Tobaria, J.J. Laserna, "Simultaneous Raman spectroscopy-laser-induced breakdown spectroscopy for instant standoff analysis of explosives using a mobile integrated sensor platform," Anal. Chem. **82(4),** 1389-1400 (2010).
[9] J.C. Carter, S. M. Angel, M. Lawrence-Snyder, J. Scaffidi, R. E. Whipple, and J. G. Reynolds, "Standoff detection of high explosive materials at 50 meters in ambient light conditions using a small Raman instrument," Appl. Spectrosc. **59,** 769–775 (2005).
[10] D. Lubczyk, C. Siering, J. Lörgen, Z.B. Shifrina, K. Müllen, S.R. Waldvogel, "Simple and sensitive online detection of triacetone triperoxide explosive," Sensors and Actuators B **143,** 561–566 (2010).
[11] M.E. Germain, M.J. Knapp, "Optical explosives detection: from color changes to fluorescence turn-on," Chem. Soc. Rev., **38,** 2543 – 2555 (2009).
[12] V. Swayambunathan, G. Singh, and R. C. Sausa, "Laser photofragmentation-fragment detection and pyrolysis-laser induced fluorescence studies on energetic materials," Appl. Opt. **38,** 6447–6454 (1999).
[13] S.J. Toal, W.C. Trogler, "Polymer sensors for nitroaromatic explosives detection," J. Mater. Chem., **16,** 2871 – 2883 (2006).
[14] I. Cotte-Rodríguez, H. Chen, R.G. Cooks, "Rapid trace detection of triacetone triperoxide (TATP) by complexation reactions during desorption electrospray ionization," Chem. Commun., 953-955 (2006).
[15] D.R. Justes, N. Talaty, I. Cotte-Rodriguez, R.G. Cooks, "Detection of explosives on skin using ambient ionization mass spectrometry," Chem. Commun., 2142-2144 (2007).
[16] C. M. Wynn, S. Palmacci, R. R. Kunz, and M. Rothschild, "Noncontact detection of homemade explosive constituents via photodissociation followed by laser-induced fluorescence," Opt. Express **18**, 5399-5406 (2010)
[17] S. Singh, "Sensors-An effective approach for the detection of explosives," J. Hazard. Mater. **144**, 15–28 (2007).
[18] W. Schade, C. Bohling, K. Hohmann, and D. Scheel, "Laser-induced plasma spectroscopy for mine detection and verification," Laser and Particle Beams **24(02),** 241–247 (2006).
[19] L.J. Radziemski, "Review of selected analytical applications of laser plasmas and laser ablation, 1987-1994," Microchem. J. 50(3), 218–234 (1994)
[20] F.C. DeLucia, A. C. Samuels, R. S. Harmon, R. A. Walters, K. L. McNesby, A. LaPointe, R. J. Winkel, and A. W. Miziolek, "Laser-induced breakdown spectroscopy (LIBS): a promising versatile chemical sensor technology for hazardous material detection," IEEE Sens. J. 5(4), 681–689 (2005).
[21] D.A. Rusak, B. C. Castle, B. W. Smith, and J. D. Winefordner, "Fundamentals and applications of laser-induced breakdown spectroscopy," Crit. Rev. Anal. Chem. **27,** 257–290 (1997).
[22] V. Lazic, A. Palucci, S. Jovicevic, C. Poggi, E. Buono, "Analysis of explosive and other organic residues by laser induced breakdown spectroscopy," Spectrochim. Acta - Part B Atomic Spectroscopy **64(10),** 1028-1039 (2009).
[23] E.G. Snyder, C. A. Munson, J. L. Gottfried, F. C. De Lucia, Jr., B. Gullet, A. W. Miziolek, "Laser induced breakdown spectroscopy for the classification of unknown powders," Appl. Opt., **47,** G80 (2008).
[24] E.L. Gurevich and R. Hergenröder, "Femtosecond Laser-Induced Breakdown Spectroscopy: Physics, Applications, and Perspectives," Appl. Spectrosc. **61**, 233A-242A (2007)
[25] C. Lopez-Moreno, S. Palanco, J. Javier Laserna, F.C. DeLucia, A.W. Miziolek, J. Rose, R.A. Walters, and A.I. Whitehouse, "Test of a stand-off laser-induced breakdown spectroscopy sensor for the detection of explosives residues on solid surfaces," J. Anal. At. Spectrom., **21(1),** 55-60 (2006).
[26] F.C. De Lucia, Jr., R.S. Harmon, K.L. McNesby, RJ. Winkel, Jr., and A.W. Miziolek, "Laser-Induced Breakdown Spectroscopy Analysis of Energetic Materials," Appl. Opt. **42**, 6148-6152 (2003).
[27] J.L. Gottfried, F.C. De Lucia Jr., C.A. Munson, A.W. Miziolek, "Double-Pulse Standoff Laser-Induced Breakdown Spectroscopy for Versatile Hazardous Materials Detection," Spectrochim. Acta, Part B, **62(12),** 1405-1411 (2007)
[28] J.L. Gottfried, F.C. De Lucia Jr, C.A. Munson, and A.W. Miziolek, "Standoff Detection of Chemical and Biological Threats Using Laser-Induced Breakdown Spectroscopy," Appl. Spectroscopy, **62(4),** 353-363 (2008).

[29] R. González, P. Lucena, L.M. Tobaria, J.J. Laserna, "Standoff LIBS detection of explosive residues behind a barrier," J. Analy. Atom. Spectrom. **24(8)**, 1123-1126 (2009).
[30] C.A. Munson, J.L. Gottfried, F.C. De Lucia Jr, and A. Miziolek, "Detection of indoor chemical and biological hazards using the man-portable laser-induced breakdown spectrometer (MP-LIBS)," Appl. Opt., **47,** G48 (2008).
[31] F. C. De Lucia, Jr., J. L. Gottfried, A. W. Miziolek, "Evaluation of femtosecond laser-induced breakdown spectroscopy for explosive residue detection," Opt. Expr. **17,** 419-425 (2009).
[32] V.I. Babushok, F.C. Delucia Jr, P.J. Dagdigian, J.L. Gottfried, C.A. Munson, M.J. Nusca, A.W. Miziolek, "Kinetic modeling study of the laser-induced plasma plume of cyclotrimethylenetriamine (RDX)", Spectrochimica Acta Part B, **62**, 1321-1328 (2007).
[33] Y. Dikmelik, C. McEnnis, and J. B. Spicer, "Femtosecond and nanosecond laser-induced breakdown spectroscopy of trinitrotoluene," Opt. Expr. **16**, 5332-5337 (2008).
[34] Y. Dikmelik, C. McEnnis, and J. B. Spicer, "Femtosecond laser-induced breakdown spectroscopy of explosives," Proc. SPIE, **6217 II,** 62172A (2006).
[35] Y. Dikmelik, J. B. Spicer, "Femtosecond laser-induced breakdown spectroscopy of explosives and explosive-related compounds," Proc. SPIE, **5974 II,** 757-761 (2005).
[36] D. Díaz, D.W. Hahn, A. Molina, "Laser induced breakdown spectroscopy (LIBS) for detection of ammonium nitrates in solids," Proc. SPIE **7303**, 73031E (2009).
[37] V. Margetic, A. Pakulev, A. Stockhaus, M. Bolshov, K. Niemax, R. Hergenröder, "A comparison of nanosecond and femtosecond laser-induced plasma spectroscopy of brass samples," Spectrochim. Acta, Part B **55**, 1771-1785 (2000).
[38] M. Baudelet, L. Guyon, J. Yu, J. P. Wolf, T. Amodeo, E. Frejafon, and P. Laloi, "Femtosecond time-resolved laser-induced breakdown spectroscopy for detection and identification of bacteria: a comparison to the nanosecond regime," J. Appl. Phys. **99**, 084701 (2006).
[39] M. Baudelet, L. Guyon, J. Yu, J. P. Wolf, T. Amodeo, E. Frejafon, and P. Laloi, "Spectral signature of native CN bonds for bacterium detection and identification using femtosecond laser-induced breakdown spectroscopy," Appl. Phys. Lett. **88**, 063901 (2006).
[40] F.C. De Lucia Jr., J.L. Gottfried, C.A. Munson, A.W. Miziolek, "Double pulse laser-induced breakdown spectroscopy of explosives: Initial study towards improved discrimination," Spectrochim. Acta, Part B, **62(12),** 1399-1404 (2007).
[41] J.L. Gottfried, F.C. De Lucia Jr., C.A. Munson, and A.W. Miziolek, "Strategies for residue explosives detection using laser-induced breakdown spectroscopy," J. Anal. At. Spectrom., **23,** 205-216 (2008).
[42] F.C. De Lucia Jr, J.L. Gottfried, C.A. Munson, and A. Miziolek, "Multivariate analysis of standoff laser-induced breakdown spectroscopy spectra for classification of explosive-containing residues," Appl. Opt., **47,** G112 (2008).
[43] http://physics.nist.gov/PhysRefData/ASD.
[44] M. Weidman, M. Baudelet, M. Fischer, C. Bridge, C.G. Brown, M. Sigman, P.J Dagdigian, M.C. Richardson, "Molecular signal as a signature for detection of energetic materials in filament-induced breakdown spectroscopy," Proc. SPIE, **7304**, 73041G-1 (2009).
[45] C. McEnnis, J. B. Spicer, "Substrate-related effects on molecular and atomic emission in LIBS of explosives," **6953,** 695309 (2008).
[46] C.G. Brown, M. Baudelet, C. Bridge, M.K. Fisher, M. Sigman, P.J. Dagdigian, M. Richardson, "Atmosphere issues in detection of explosives and organic residues," Proc. SPIE **7304,** 73041D (2009).
[47] A. Khachatrian and P. J. Dagdigian, "Laser-induced breakdown spectroscopy with laser irradiation on mid-infrared hydride stretch transitions: polystyrene," Appl. Phys. B 97(1), 243–248 (2009).
[48] S. Wallin, A. Pettersson, H. Östmark, A. Hobro, "Laser-based standoff detection of explosives: a critical review," Anal. Bioanal. Chem. **395**, 259–274 (2009).